INL/CON-19-56985-Revision-0

Designing an impedance-based technique for studying corrosion on cladding materials

June 2020

Ling Ding, Hongqiang Hu, Michael F. Hurley

INL/CON-19-56985-Revision-0

Designing an impedance-based technique for studying corrosion on cladding materials

Ling Ding, Hongqiang Hu, Michael F. Hurley

June 2020

Idaho National Laboratory
Idaho Falls, Idaho 83415

http://www.inl.gov

Prepared for the
U.S. Department of Energy
Under DOE Idaho Operations Office
Contract DE-AC07-05ID14517

Designing an impedance-based technique for studying corrosion on cladding materials

Ling Ding, * Hongqiang Hu[†], Michael F. Hurley[††]

*Idaho National Laboratory, 2525 Fremont Ave, Idaho Falls, ID 83415, USA, Ling.Ding@inl.gov
[†]Idaho National Laboratory, 2525 Fremont Ave, Idaho Falls, ID 83415, USA, Hongqiang.Hu@inl.gov
[††]Micron School of Materials Science and Engineering, Boise State University, 1910 University Dr, Boise, Idaho 83725-2075, mikehurley@boisestate.edu

INTRODUCTION

In nuclear cladding materials, changes in structure and chemistry over the lifetime of claddings can have a significant impact on fuel and reactor performance. Currently, chemical evolution over the lifetime of the fuel and cladding materials can only be inferred using post-irradiation examination. As an alternative to post-irradiation measurements, electrochemical impedance spectroscopy (EIS) can provide an in-pile measurement of changes in chemistry in oxides and hydrides.

The objective of this study is to develop an impedance based sensing technology for measuring spatial- and time-resolved in-pile changes in cladding chemistry in order to understand the mechanisms of hydride formation, hydride dealloying and associated cladding corrosion so that a mitigation strategy and technology can be developed for reactor safe operation. Two prototype impedance-based sensors were designed and assembled using Zr-4 as working electrode and Pt as counter and reference electrode. One sensor is tubular type and the other one is plate-type. These sensors will be tested in static autoclave to investigate the effects of various environmental conditions (including temperature, pressure, and water chemistry) on cladding material corrosion mechanisms. These in-situ EIS sensors would provide corrosion-layer parameters in high-temperature water, such as (1) total layer thickness, (2) the evolution of oxide structures as uniform layer dielectric or sublayer(s), and (3) the possible electrochemistry of the volume corrosion process and the solid/liquid interface, such as the cyclic nature of corrosion of Zr alloys in high-temperature water.

This work was focused on electrochemical sensor development, targeting cladding oxides/hydrides under thermodynamic equilibria; characterization of samples using Kelvin probe force microscopy (SKPFM), Raman spectroscopy, and scanning electron microscopy (SEM) with energy-dispersive X-ray spectroscopy (EDS) to provide high-resolution co-localized characterization of zirconium oxide and metal/oxide interface.

EIS Sensor Development for Static Autoclave

Two Zr-4 materials were used in this study for designing EIS sensors with composition listed in Table 1: Zr-4 alloy tube (ID 1.524cm and thickness 0.254cm) and Zr-4 sheet (thickness 0.318cm) from American Elements (Product No.: Zr-Ally-Za4-She). The compositions for the two Zr-4 materials are very similar. Zr content is higher than 98% for both materials. Ceramic tubes (Coorstek) are single bore open end tubes with 0.318cm OD. Pt wire (California Fine Wire) is pure TC grade with 0.05cm diameter. Pt mesh (American Elements) is 52x52 mesh with 0.01cm ID. And the thickness of Pt sheet (Surepure Chemicals) is 0.1 mm. Two types of EIS sensors (plate- and tubular-type) were designed and assembled according to the diagram shown in Figure 1. A ceramic bond (Aremco, new Ceramabond 552) was used to glue ceramic tubes and metal material together. And silver ink (Fuel Cell Materials, AG-I) was used for holding Pt wires. The designed EIS sensors were planned to be tested in a static autoclave. A Parr Instruments Series 4570 High Pressure / High Temperature (HP/HT) Reactor (Parr reactor) is used as the static autoclave in this study (Figure 2).

Table 1. Zirconium alloy compositions.

(wt %)	Zr	Sn	Fe	Cr	O	Si	Al	Ni	Ti	Cu
Zr-4 Tube	98.18	1.4	0.2	0.1	0.12	—	—	—	—	—
Zr-4 sheet	98.23	1.44	0.2	0.1	—	0.0062	0.0093	0.0018	0.0013	0.0025

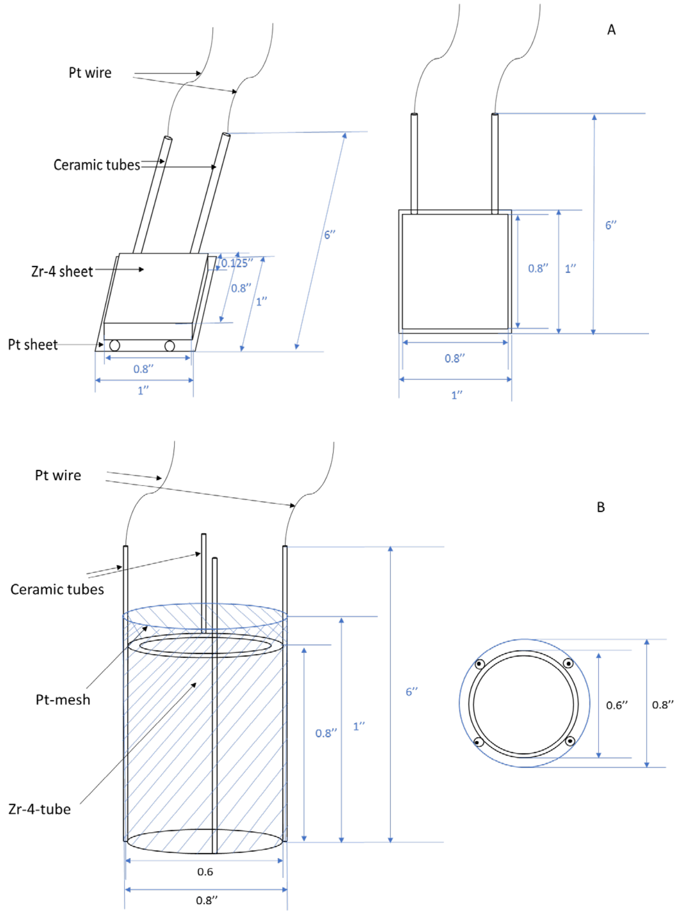

Figure 1. EIS sensor diagram. (A) plate-type; (B) tubular-type.

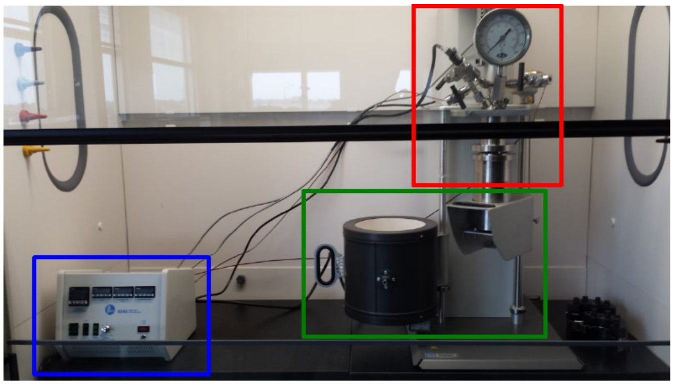

Figure 2. The main components of the Parr reactor system are illustrated in the red box - reaction vessel, green box - heating mantle, blue box - controller. Actual system configuration can vary slightly and will be managed in the lab notebook. Other components could include a circulating bath for reactor cooling.

EIS Testing of Zr-4 in High-Temperature/Pressure water (250 °C/573 Psi)

Even though in-service conditions will be at higher temperature and with irradiation, the autoclave testing provides prototypical sensor signals to aid with calibration of the sensor and initial data to develop procedures for interpreting the sensor signals that must be correlates with physical conditions. Autoclave testing also allows easy post-testing verification of the sample and sensor conditions to help validate sensor signal correlations with physical process. This work is essential development work towards implementing a robust in-core EIS sensor.

Zr-4 sensors as shown in Figure 1 were used for this work, with their respective compositions shown in Table 1. Oxygen free-pressurized water at 250 °C in a static autoclave (pressure 570 psi) was used. The experiment was continuous during the first 40 days. EIS tests were carried out using the 10 mV AC sinusoidal perturbation potential with the frequency from 1 MHz to 0.01 Hz with 6 frequencies per decade.

Figure 3 presents typical Nyquist and Bode plots reported at various exposure time. It can be seen that the formation of the oxide caused a rapid increase of the impedance and the character of the impedance spectra changed in the course of corrosion process. Two to three time constants are distinguishable in the spectra-a high frequency one is ascribed to the dielectric response of the oxide, while the low frequency ones involve faradic phenomena-mass and charge transfer at the interface [1]. As the oxide layer thickness increases, its capacitance decreases and the high frequency relaxation time constant moves to higher frequencies. At the same time faradic time constants move to lower frequencies, mostly due to an increase in diffusion impedance.

The number of time constants increase was observed after one week of exposure. A two-time constant developed in the impedance spectra at the short exposure time and three-time constants developed in the long exposure time (Figure 4). Therefore, the different stages of the corrosion process could not be approximated using a single model of equivalent circuit. The constant phase element, CPE, is more flexible for approximation of the dispersive impedance data than the “ideal” capacitance, C [2]. An equation that describes impedance of the constant phase element is presented in Eq. (1)[3].

$$Z_{CPE} = Q^{-1}(j\omega)^{-n} \qquad (1)$$

Where Q is CPE coefficient and n is CPE exponent with $0<n<1$. The exponent n is a measure of the capacitance dispersion. The coefficient Q has the dimension of capacitance when n=1, of resistance when n=0 and of the Warburg impedance, W, when n=0.5. An equation that implies relationship of the oxide thickness, d_{ox}, and non-ideal capacitance of oxide, Q_{ox}, is present as Eq. (2).

$$d_{ox} \sim Q_{ox}^{-1} \qquad (2)$$

The thickness of the oxide was not quantitively calculated and the relation presented in Eq. (2) was only used to show the qualitative evolution of the barrier oxide. In this manner the EIS is used as a non-destructive technique that permits in-situ, real-time, and historical data to be obtained.

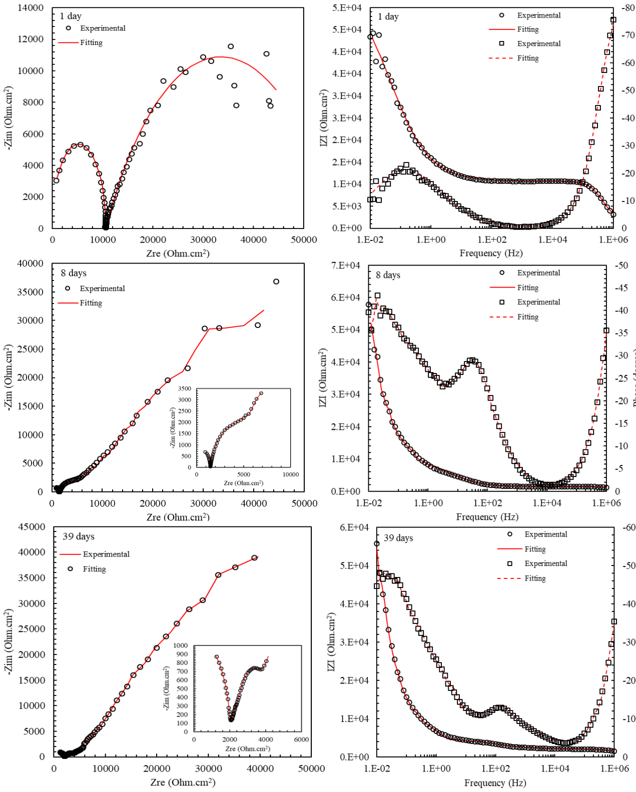

Figure 3. Time evolution of impedance spectra of Zr-4 sensors over the exposure.

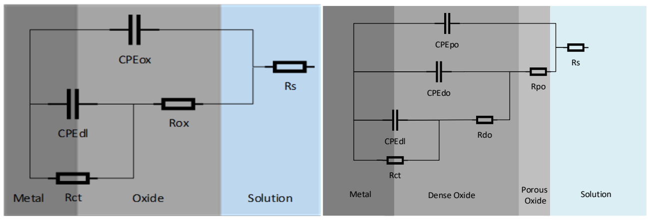

Figure 4. Models of equivalent circuits; R_s is the solution resistance, R_{ox} is the oxide resistance, R_{po} is the resistance of porous oxide layer, R_{do} is the resistance of dense oxide layer, R_{ct} is the charge transfer resistance, CPE_{ox} is the non-ideal oxide capacitance and CPE_{dl} is non-ideal capacitance of the double layer.

Co-localization SKPFM, Ramen and SEM/EDS

Co-localized SKPFM, Raman mapping, and SEM/EDS was performed on the sectioned Zr-4 sample. There is an area of lower percent tetragonality at the metal/oxide interface with similar shape and size to the cathodic particle, a closer look at this particle is seen in Figure 5. Co-localization of X-Y position for each technique was accomplished based on the distance from the metal/oxide interface to other notable features. The Volta potential for the particle is ~600 mV greater than the neighboring metal, displaying relative cathodic nature (Figure 5a). This particle's Volta potential maximum is at the same point as the largest compressive stress (Figure 5c, as it relates to a decrease in M2 peak position). Additionally, this occurs when percent tetragonality is increasing, but is still below its maximum value (Figure 5b). The end of the oxide, where percent tetragonality and M2 peak position lines abruptly end, is where the particle ends, and the metal interface begins in terms of Volta potential. For compositional correlation, a line scan of EDS measurements is included (Figure 5d). Further evidence of either nitride or iron-enrichment for this particle can be seen in Figure 6, showing individual Raman spectra across a portion of the noted line scan in Figure 5. There is no discernable evidence of concentrated iron or nitrogen counts near the metal/oxide interface. A possible reason for this lack of secondary element response may be due to the damage inflicted upon the sample from the 50 mW Raman laser. When laser power is increased, there is a tradeoff between maximizing signal and increasing surface damage. Damage to the sample surface from the Raman laser makes it difficult to resolve particles even a few microns in size with SEM/EDS.

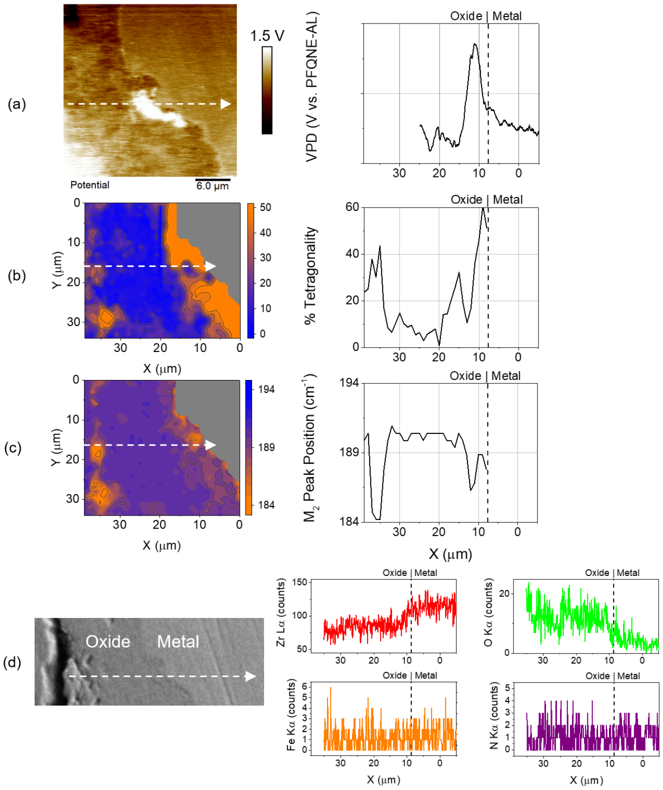

Figure 5. Co-localization between (a) SKPFM Volta potential map with VPD line scan of 1 V range, (b) percent tetragonality and (c) M2 peak position maps with line scans

determined via Raman mapping, and (d) SEM image with EDS elemental line scans for a sectioned sample of oxidized Zr.

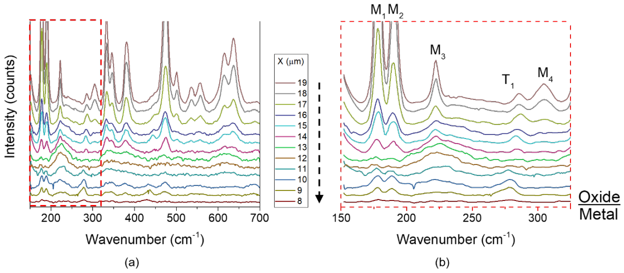

Figure 6. (a) Raman spectra for partial distance across the line scan in Figure 5. (b) Inset of spectra with monoclinic (M) and tetragonal (T) zirconia peaks noted.

RESULTS

Two prototype impedance-based sensors were designed and assembled using Zr-4 as working electrode and Pt as counter and reference electrode. One sensor is a tubular type and the other one is a plate-type. In the future, these sensors will be tested in various facilities with different conditions, including static autoclave, flowing water autoclave, and ATR to investigate the effects of various environmental conditions (including temperature, pressure, and water chemistry) on cladding material corrosion mechanisms. These in-situ EIS sensors would provide corrosion-layer parameters in high-temperature water, such as (1) total layer thickness, (2) the evolution of oxide structures as uniform layer dielectric or sublayer(s), and (3) the possible electrochemistry of the volume corrosion process and the solid/liquid interface, such as the cyclic nature of corrosion of Zr alloys in high-temperature water.

The EIS results in autoclave conditions demonstrated that increasing samples' testing time results in more layers of passive oxide thickening with time in solution. In addition, the repeatability and effectiveness of EIS techniques to capture differences in both electrolyte and alloy composition were confirmed by experimental results. In this manner the EIS is used as a non-destructive technique that permits in-situ, real-time, and historical data to be obtained. These results all support development of the in-core sensor design and interpretation of the prototypical sensor signals.

Co-localization of SKPFM, Raman mapping, and SEM/EDS allowed correlation of different oxide and metal characteristics of Zr-4. SKPFM is a useful characterization technique to support the understanding of cladding oxidation mechanisms. This high-resolution, non-destructive technique can be used in the future for hydride detection and growth, oxide stoichiometry and phase distribution, secondary phases' role in cladding oxidation mechanisms, and irradiation effect of the cladding's electronic properties. When combined with complementary characterization techniques, the methods reported establish novel experimental advancements that can provide new insight into cladding degradation processes.

REFERENCE

[1] A. Krausova, J. Macak, P. Sajdl, R. Novotny, V. Renciukova, V. Vrtilkova, In-situ electrochemical study of Zr1nb alloy corrosion in high temperature Li+ containing water, J Nucl Mater 467 (2015) 302-310.
[2] M.E. Orazem, I. Frateur, B. Tribollet, V. Vivier, S. Marcelin, N. Pebere, A.L. Bunge, E.A. White, D.P. Riemer, M. Musiani, Dielectric Properties of Materials Showing Constant-Phase-Element (CPE) Impedance Response, J Electrochem Soc 160(6) (2013) C215-C225.
[3] V. Renciukova, J. Macak, P. Sajdl, R. Novotny, A. Krausova, Corrosion of zirconium alloys demonstrated by using impedance spectroscopy, J Nucl Mater 510 (2018) 312-321.